

# HYDRODYNAMICS OF HIGH-REDSHIFT GALAXY COLLISIONS: FROM GAS-RICH DISKS TO DISPERSION-DOMINATED MERGERS AND COMPACT SPHEROIDS

FRÉDÉRIC BOURNAUD, DAMIEN CHAPON, LAURIANE DELAYE, LEILA C. POWELL

Laboratoire AIM Paris-Saclay, CEA/IRFU/SAP – CNRS – Université Paris Diderot, 91191 Gif-sur-Yvette Cedex, France.  
 frederic.bournaud@cea.fr

BRUCE G. ELMEGREEN

IBM T. J. Watson Research Center, 1101 Kitchawan Road, Yorktown Heights, New York 10598 USA, bge@us.ibm.com

DEBRA MELOY ELMEGREEN

Vassar College, Dept. of Physics & Astronomy, Poughkeepsie, NY 12604, elmegreen@vassar.edu

PIERRE-ALAIN DUC

Laboratoire AIM Paris-Saclay, CEA/IRFU/SAP – CNRS – Université Paris Diderot, 91191 Gif-sur-Yvette Cedex, France.

ROMAIN TEYSSIER

Laboratoire AIM Paris-Saclay, CEA/IRFU/SAP – CNRS – Université Paris Diderot, 91191 Gif-sur-Yvette Cedex, France.  
 Institute for Theoretical Physics, University of Zürich, CH-8057 Zürich, Switzerland.

THIERRY CONTINI, BENOIT EPINAT

Laboratoire d'Astrophysique de Toulouse-Tarbes, Université de Toulouse, CNRS, 14 Avenue Edouard Belin, 31400 Toulouse, France.

KRISTEN L. SHAPIRO

Department of Astronomy, Campbell Hall, University of California, Berkeley, CA 94720.

*Draft version June 1, 2019*

## ABSTRACT

Disk galaxies at high redshift ( $z \sim 2$ ) are characterized by high fractions of cold gas, strong turbulence, and giant star-forming clumps. Major mergers should typically involve such galaxies. High-redshift merger simulations, however, have always modeled the ISM as stable, homogeneous, and thermally pressurized. We present the first high-redshift merger simulations with cold, turbulent, and clumpy gas, and we discuss the major new features of these models compared to models where the gas is artificially stabilized and warmed. Gas turbulence, which is already strong in high-redshift disks, is further enhanced in mergers. Some phases are dispersion-dominated, with most of the gas kinetic energy in the form of velocity dispersion and very chaotic velocity fields, unlike low-redshift mergers. High-redshift mergers are also characterized by highly dissipative gas collapse to the center of mass, with the stellar component following in a global contraction. The final galaxies are early-type with relatively small radii and high Sérsic indices, like high-redshift compact spheroids. The mass fraction in a disk component that survives or re-forms after a merger is severely reduced compared to models with stabilized gas, which lends support to cold accretion as the main formation mechanism for massive disks at high redshift.

*Subject headings:* galaxies: formation — galaxies: interactions — galaxies: high-redshift — galaxies: elliptical and lenticular, cD — galaxies: structure

## 1. INTRODUCTION

In the  $\Lambda$ -CDM cosmological model, collisions and mergers are an important growth mechanism for massive galaxies, and most of them should have occurred at high redshift ( $z > 1$ ). Fundamental properties of high-redshift mergers are however largely unknown.

First, determinations of the merger rate high-redshift surveys are usually based on irregular structures or disturbed kinematics (e.g., Conselice et al. 2003; Lotz et al. 2006; Overzier et al. 2010; Jogee et al. 2009;

López-Sanjuan et al. 2009; Puech 2010). But at high redshift, galaxies can get irregular morphology and disturbed kinematics through cold accretion and internal evolution without mergers (Bournaud et al. 2007a; Genzel et al. 2008; Bournaud et al. 2008; Dekel et al. 2009), thus the actual merger rate remains unknown.

Second, the outcome of major mergers is usually considered to be early-type galaxies (ETGs). However, high-redshift ETGs are often unexpectedly compact compared to nearby ellipticals and merger simulations (Daddi et al.

2005; Trujillo et al. 2006; van Dokkum et al. 2009). The role of mergers in forming these ETGs has been questioned.

Third, the growth of galaxies near  $L^*$  is largely through cold flow accretion (Dekel et al. 2009), but about one-third of the baryons are still expected to be provided by significant mergers (e.g., Brooks et al. 2009). Major and minor mergers can convert disks into ellipticals (Naab & Burkert 2003; Bournaud et al. 2007b). This calls the survival of disk-dominated galaxies into question (Weinzirl et al. 2009).

The dynamics and outcome of mergers have never been modeled for realistic high-redshift galaxies. Simulations by Cox (2004), Springel & Hernquist (2005), and Robertson et al. (2006) considered high gas fractions and concluded that disks could survive or re-form after a merger. However, these simulations had high thermal pressure support in the ISM (temperature  $> 10^4$  K), and this forced the gas to be smooth and stable in the galaxy collisions.

Star-forming galaxies at high redshift ( $z = 1 - 5$ ) are very different from such models. They are generally gassy, clumpy, and turbulent disk galaxies, with  $\sim 50\%$  of the baryons in cold gas (Daddi et al. 2010; Tacconi et al. 2010), giant clumps of  $10^7 - 10^9 M_\odot$  (Elmegreen et al. 2004, 2007, 2009), and velocity dispersions of several tens of  $\text{km s}^{-1}$  (Förster Schreiber et al. 2009; Shapiro et al. 2008; Genzel et al. 2008; Epinat et al. 2009). Such properties are reproduced in cosmological simulations (Agertz et al. 2009; Ceverino et al. 2010).

We present hydrodynamical AMR simulations of major mergers between galaxies with high fractions of cold, turbulent and clumpy gas, like typical  $z \sim 2$  star-forming galaxies. Gas cooling below  $10^4$  K is allowed, supersonic ISM turbulence is captured, and the main star-forming complexes are directly resolved. We compare with models using artificially stabilized disks, as in traditional high-redshift studies.

ISM turbulence and cloudiness has significant effects in low-redshift mergers (Bois et al. 2010; Teyssier et al. 2010). The effects become dramatic in high-redshift conditions. We find that mergers of high-redshift disks have a dispersion-dominated phase with very chaotic velocity fields. The merging system undergoes a rapid dissipational collapse into a compact ETG. The mass fraction in a surviving or re-formed disk component is much lower for typical high-redshift mergers than for models with artificially warmed gas.

## 2. SIMULATIONS

The simulations were performed with the AMR code RAMSES. The technique is fully described elsewhere and shown to model realistic interstellar gas in low-redshift mergers and isolated disks (Teyssier et al. 2010; Bournaud et al. 2010). The main parameters adopted for the present simulations are in Table 1.

The box size for the simulation is 200 kpc. The coarsest level of the AMR grid is  $l = 8$ , which corresponds to a  $256^3$  Cartesian grid with a cell size of 781 pc. A cell that contains a gas mass larger than  $m_{\text{res}} = 8 \times 10^4 M_\odot$ , or a number of particles larger than 15, is refined, until the maximal level  $l = 11$  is reached. At that point, the cell size corresponds to 97 pc. Stars and dark matter are

described with  $2 \times 10^5$  collisionless particles each in the initial galaxies.

Our clumpy disk simulations were performed with a barotropic cooling model (Teyssier et al. 2010; Bournaud et al. 2010), naturally producing a cloudy and turbulent ISM, with a temperature floor around  $10^3$  K. We refer to these as the *cooling* models. For comparison, the same gas-rich mergers were modeled with a thermally pressurized and Toomre-stable ISM, using an adiabatic Equation of State (EoS) with an exponent of  $\gamma = 5/3$  for densities above  $1 \text{ cm}^{-3}$ , and  $T = 10^4$  K for lower densities. This EoS maintains a Toomre parameter  $Q \simeq 1.5 - 2$  in the initial disks and stabilizes the gas against axisymmetric perturbations. These will be called the *stabilized* models. In all cases, a density-dependent temperature floor ensures that the Jeans length is resolved by at least 4 cells to avoid artificial fragmentation, as in Teyssier et al. (2010).

In the cooling models, star formation is assumed to proceed above a density threshold of  $300 \text{ cm}^{-3}$  with an efficiency of 7%, i.e. 7% of the gas in a given cell forms stars per local free-fall time. This gives an SFR of  $120 M_\odot \text{ yr}^{-1}$  in the isolated disk model, realistic for such gas-rich  $z \sim 2$  systems. In the stabilized models, the star formation threshold is  $3 \text{ cm}^{-3}$  and the efficiency is 4%, giving the same SFR in the isolated disks: we compare the two sets of models with the same SFR in pre-merger disks.

All simulations use the kinetic feedback model described in Dubois & Teyssier (2008), with 20% of the energy from each supernovae re-injected in the form of an expanding bubble of initial radius 100 pc. One model has increased feedback with 100% of the supernova energy injected into the ISM.

Our simulations start with disks containing baryonic masses of  $8 \times 10^{10} M_\odot$ , initial gas fractions of 70%, a disk scale length of 5 kpc with a truncation radius of 12 kpc, and an initial scale-height of 800 pc. An initial bulge containing 15% of the stellar mass is assumed, with a Hernquist profile and a scale-length of 500 pc. The dark matter halo has a Burkert profile with a core radius of 8 kpc, and a mass fraction (dark/total) inside the disk radius of 30%. The circular velocity in the outer disk is  $245 \text{ km s}^{-1}$ .

In the cooling models, the initial disks spontaneously become clumpy and turbulent, with  $V/\sigma \simeq 5$  (for rotation speed  $V$  and turbulent speed  $\sigma$ ) and gas fraction around 50 % (after some early gas consumption) when the interaction begins, as expected for a wet merger at  $z \sim 2$ .

We used relatively massive and extended initial galaxies, so as to compare with existing models, e.g., Robertson et al. (2006). There are galaxies like this in  $z \sim 2$  samples, and extension to lower masses is discussion in Section 4. Also, our pre-merger disks are not extreme in terms of gas clumpiness and turbulence: many  $z \sim 2$  disks have even lower  $V/\sigma$  ratios (e.g., Förster Schreiber et al. 2009).

Three interaction orbits were used. They are all prograde for one galaxy and retrograde for the other in order to consider a typical total angular momentum rather

TABLE 1  
PARAMETER USED FOR THE SIMULATIONS, AND PROPERTIES OF THE FINAL RELAXED SYSTEM:

Half-mass radius  $R_{1/2}$ , Sersic index  $n$  (best fit between 0.3 and  $3 R_{1/2}$ ), and baryonic mass fraction of the baryons in a rotating disk  $f_{\text{disk}}$  (from a kinematic disk+spheroid decomposition).

Model	Orbit	Model parameter		Merger remnant properties		
		EoS	Comment	Sersic $n$	$R_{1/2}$	$f_{\text{disk}}$
C1	1	cooling	merger of gas-rich clumpy disks	4.4	2.8	12%
C1F	1	cooling	C1 with stronger feedback	4.2	3.0	16%
S1	1	stabilized	gas-rich, smooth, stabilized disks	2.9	6.1	40%
C2	2	cooling	merger of gas-rich clumpy disks	4.2	2.9	14%
S2	2	stabilized	gas-rich, smooth, stabilized disks	3.2	5.8	37%
C3	3	cooling	merger of gas-rich clumpy disks	4.9	2.6	11%
S3	3	stabilized	gas-rich, smooth, stabilized disks	3.3	5.6	37%
I	isolated	cooling	control run: high-redshift disk	1.7	5.4	66%

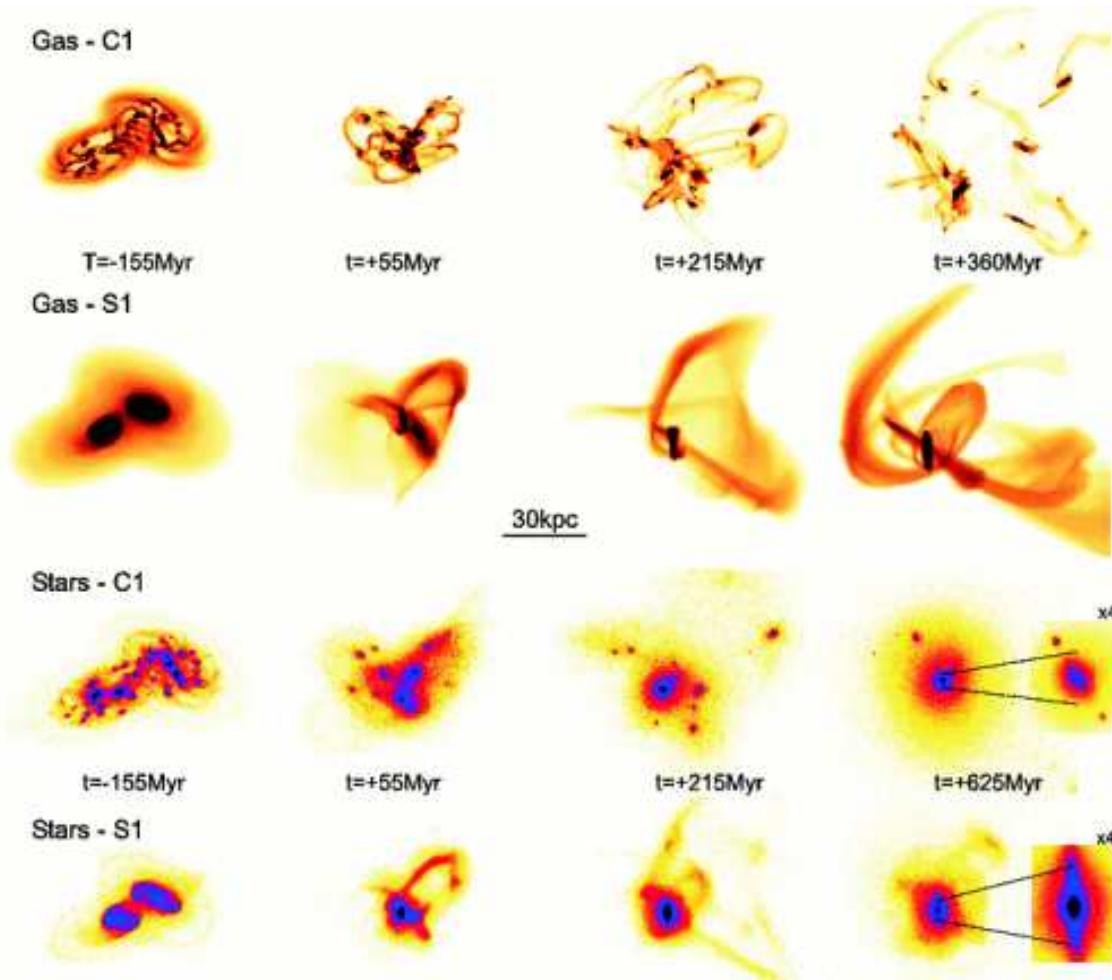


FIG. 1.— Snapshots of the gas and total stellar mass distribution for models C1 (cooling) and S1 (stabilized) at similar instants and under similar projections.  $t = 0$  is the first pericenter passage and all maps are in log scale.

than extreme cases with aligned spins<sup>1</sup>. Orbit 1 has an impact parameter of 12 kpc and is parabolic. One disk has an initial inclination of  $30^\circ$  from the orbital plane, and the other has an initial inclination of  $50^\circ$ . For orbit 2, these parameters are: 35 kpc, hyperbolic (total energy of the galaxy pair is 0.3 times its initial kinetic energy), and  $30^\circ$  and  $50^\circ$  degrees, respectively. For or-

bit 3, they are 25 kpc, hyperbolic (total energy =  $0.2 \times$  the initial kinetic energy),  $40^\circ$ , and  $65^\circ$  degrees, respectively.

### 3. RESULTS

#### 3.1. On-going mergers

The time evolution of mergers C1 (cooling) and S1 (stabilized) is shown in Figure 1. The stabilized model has relatively homogeneous tidal tails orbiting around two, then one, relatively smooth gas disks. The gas in the

<sup>1</sup> Aligned spins would not result in higher angular momentum or more disk component in the final result, because of tidal removal of the angular momentum (Robertson et al. 2006)

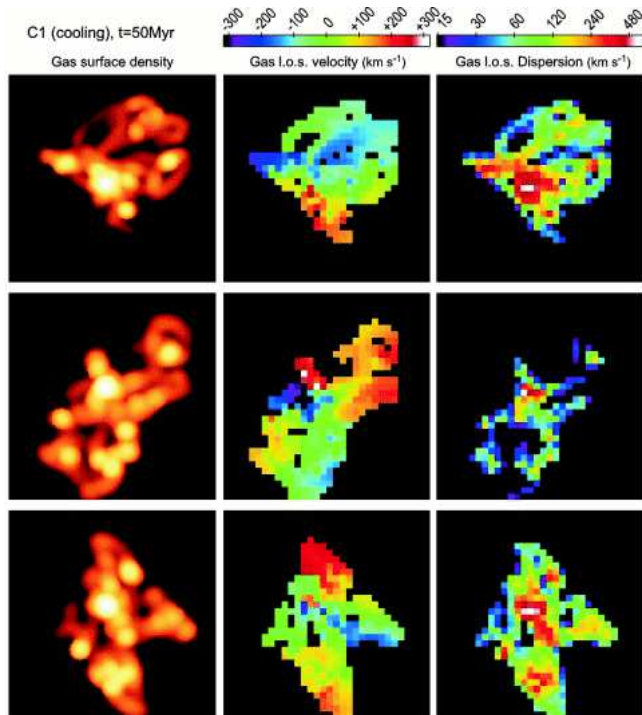


FIG. 2.— Three orthogonal projections of model C1 showing the surface density, and velocity and dispersion maps (mass-weighted values along the line-of-sight, for gas denser than  $10 \text{ cm}^{-3}$ ). A resolution of  $1 \text{ kpc}$  was assumed (FWHM of a gaussian beam). All snapshots are  $44 \times 44 \text{ kpc}$ . Note that  $\text{H}\alpha$  observations would be mostly sensitive to emission from the dense clumps.

cooling model is dominated by numerous star-forming clumps that are somewhat more massive than the clumps were in the pre-merger galaxies. Visual inspection shows that some of the pre-existing clumps survived and some have disrupted and re-formed. Numerous filaments form in many directions, instead of a main pair of continuous tidal tails. Other projections (Fig. 2) show that the gas distribution during the merger forms a very irregular spheroid in three dimensions; there are no disks. The model with stronger feedback (C1F in Fig. 3) is qualitatively similar: self-gravity is already sufficient drive strong ISM turbulence in massive galaxies at high redshift (Dekel et al. 2009; Elmegreen & Burkert 2010).

Gas velocity fields and line-of-sight dispersion maps are shown in Figures 2 and 3. The gas velocity fields of our high-redshift cooling models are very chaotic, and often lack extended rotating components, such as large disks or long tidal tails with monotonic velocity gradients. The gas velocity dispersions are high, especially near dense clumps.

Interactions at low redshift substantially increase the gas velocity dispersion, from typically  $10 \text{ km s}^{-1}$  in non-interacting spirals to  $30\text{--}40 \text{ km s}^{-1}$  in major mergers (see Elmegreen et al. 1995 for observations, Bournaud et al. 2008 for simulations). We find a similar relative increase here, but starting with disks that are already quite turbulent before the merger. This results in systems where the gas component is dispersion-dominated during the merger, with  $V/\sigma$  ratios<sup>2</sup> of around 2 or even 1 for some

<sup>2</sup> Throughout the paper,  $\sigma$  refers to a one-dimensional dispersion. A system with  $V/\sigma < 2$  is dispersion-dominated with  $> 60\%$  of its kinetic energy support is in the form of dispersions.

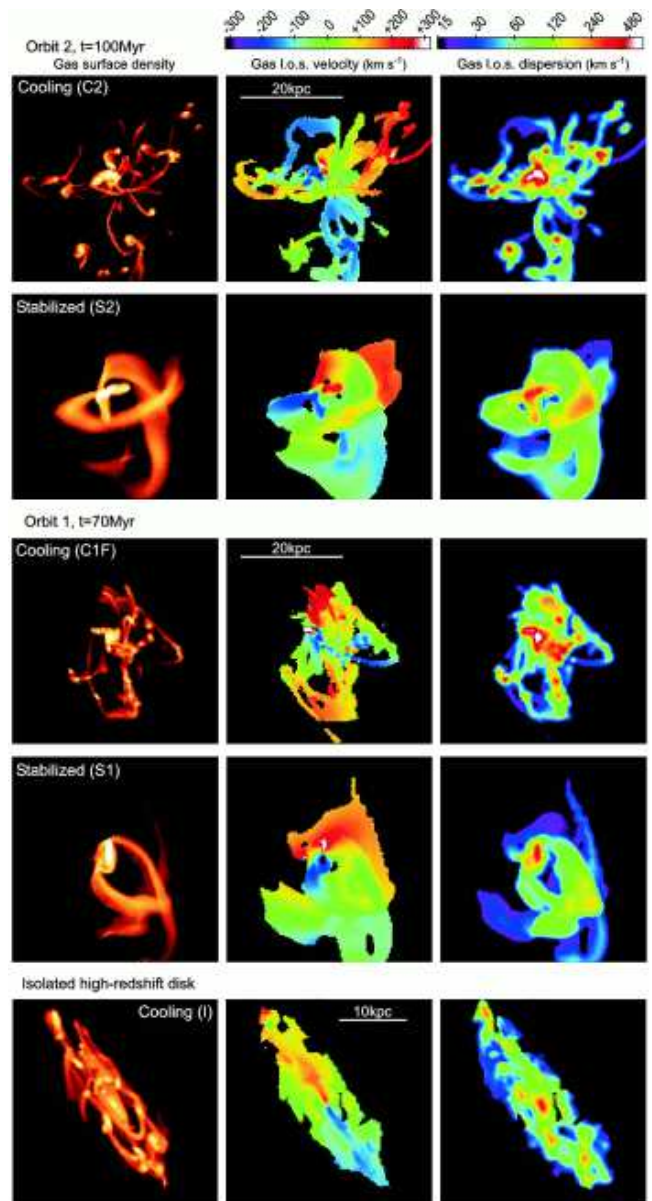


FIG. 3.— Same as Fig. 2, with comparison of on-going mergers in the cooling and stabilized models at the same instant and under the same projection, shown here at full resolution. An isolated clumpy turbulent disk is also shown after a similar evolutionary time as the mergers.

projections and times. The gas dispersions are high in projection on the line-of-sight, and also in direct measurements of the local three-dimensional motions: we measured the turbulent velocity dispersion in  $1 \text{ kpc}^3$  cubes in model C1 at  $t = 140 \text{ Myr}$ ; the mass-weighted average value was  $< \sigma_{\text{turb, 1D}} > \approx 175 \text{ km s}^{-1}$ .

Mergers with the stabilized ISM model show velocity dispersions that are lower by a factor  $\sim 3$  for all times. Instead of chaotic velocity fields, they have relatively smooth and extended rotating gas disks, surrounded by long tidal tails that co-rotate with large-scale velocity gradients (see examples in Fig. 3). Such morphological and kinematical signatures are observed for low redshift mergers (see examples in Bournaud et al. 2004; Chilingarian et al. 2010). The low-redshift ISM is more stable (on large scales), less turbulent, and stabi-



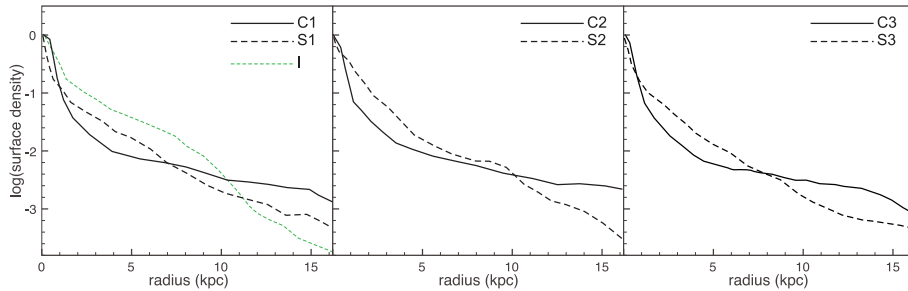


FIG. 4.— Radial profiles of the stellar surface densities in final merged and relaxed systems, and the isolated disk model after the same evolutionary time. Several projections were averaged for each model. Ellipse-fitting was performed with the `ellipse` task in `IRAF`.

lized high-redshift models resemble this.

### 3.2. Merger remnants

Supersonic gas turbulence dissipates rapidly, which can produce a strong contraction of a dispersion-supported gaseous system. Such dissipative collapse is observed in Figure 1 for model C1. Some clumps are expelled by tidal interactions, but most of the gas clumps and inter-clump gas coalesce in a compact central object. Because the gas fraction is initially high, a large part of the final stellar content forms within the same gas clumps and follows their coalescence. Old stars also contract as the gas and young stars contain a large fraction of the total mass. Thus, the merger leads to the formation of a relatively compact stellar spheroid. This spheroid has a low half-mass radius, a high Sersic index, and an extended stellar halo. Table 1 gives half-mass radii and Sersic indices for all models. Figure 4 shows the corresponding stellar mass profiles. Remnants of the stabilized merger models are more extended and have lower Sersic indices than remnants of the cooling merger models. The isolated clumpy turbulent disk model has formed a central bulge through internal evolution, but remains dominated by a rotating exponential disk (Bournaud et al. 2007a).

The merger remnant of a typical high-redshift merger is not just more compact, but also less disk. Gas re-growth is faster in the models with a stabilized ISM (see Fig 1 at  $t = 215$ ), and thus forms a more massive final stellar disk. For example, the final disk component in model S1 contains 40% of the baryons and is obvious up to large radius in Figure 1. In cooling model C1, most star formation takes place in gas clumps before they coalesce and get a chance to re-form a disk, the final disk in model C1 is compact, with a disk fraction of only 12%. Similar differences are found for all orbits (Table 1).

The increased dissipation and resulting compactness in models with a clumpy turbulent gas can be explained: clumps interact with each other gravitationally, scatter, and develop 3D motions (i.e., high dispersions). The gas clumps and holes can then pass by each other, whereas in smooth distributions the gas cannot pass through itself and therefore rapidly settles back in relatively planar disks. Gas clumpiness could reduce the cross section and increase the dissipation timescale, but supersonic turbulence is a dissipative support. This is unlike stabilized models, where the gas is supported by a thermal pressure: thermal energy could be radiated away, but the EoS, high temperature floor, and/or feedback recipe, keep the gas warm in these models and make the thermal support non-dissipative in practice. Furthermore, mas-

sive clumps in turbulent high-redshift gas can rapidly migrate inwards through dynamical friction, unlike the relatively homogeneous gas in stabilized models.

## 4. DISCUSSION

### 4.1. Clumpy merger morphologies

The stellar distribution in our models shortly after the pericenter resembles a single “clumpy galaxy”, but it is more asymmetrical than the pre-merger clumpy disk models (see second and third panels in Figure 1). This could be consistent with the population of “assembly galaxies” in Elmegreen et al. (2007), with entirely clumpy morphologies not consistent with their being isolated disks. Other examples of high-redshift clumpy mergers can be found in Lotz et al. (2006).

### 4.2. Kinematical signatures

The mergers modeled here in realistic high-redshift conditions resemble some dispersion-dominated systems (DDS) observed in  $z \sim 2$  surveys. To further probe whether such mergers would be easily identified in observations, three of us (TC, BE, KS) performed a blind classification of the velocity and dispersion fields from Figure 2 with gas density maps, and from Figure 3 without the density maps. The test was done without knowledge on the nature of the modeled systems. Model I is recognized as an isolated disturbed disk, with some suggestions that the top-left clump could be a minor merger. The stabilized merger models are most often identified as mergers (two-thirds of the votes), generally with a high confidence level that these are binary major mergers. The cooling merger models were classified as DDS of unclear nature (about one-third of the votes), DDS of merger origin (one-third), and merger (one-third); more than half of the votes suggesting a merger or DDS merger suggested a group or multiple merger rather than a binary major merger. This confirms that (i) on-going mergers with clumpy turbulent gas could be classified as DDS, and (ii) typical high-redshift mergers have substantially different kinematics from low-redshift mergers or models with artificially stabilized gas.

Many observed DDS have small sizes, so the high observed dispersions could sometimes result from blending at low resolution, but seem in general real (Law et al. 2009). There are nevertheless DDS that are relatively massive, extended, with chaotic velocity fields. Examples include Q1623-BX453, Q17000-BX710, and others in Law et al. (2009) and in Förster Schreiber et al. (2009). These could be major mergers of initially clumpy and turbulent galaxies, but that their merger nature has not

been clearly recognized yet because they lack the usually known signatures of mergers.

Disk galaxies with lower masses than in our present models tend to be even more turbulent (lower  $V/\sigma$ , Förster Schreiber et al. 2009, e.g.). Reaching dispersion-dominated phases in mergers of such galaxies could be even easier. This might explain why observed DDS generally have small stellar masses, even though they are too numerous to all be major mergers. Overall, DDS are generally suggested to result from violent gassy collapse (Law et al. 2009), which our models show can occur in high-redshift mergers.

#### 4.3. High-redshift ETGs

Our merger models with cooling predict final stellar distributions that are relatively compact. The properties of the final ETGs in our cooling models are comparable to the three most compact high-redshift ETGs in the Mancini et al. (2010) sample with similar masses, as well as some objects in Cappellari et al. (2009). Mergers with various mass ratios, gas fractions, and levels of ISM turbulence could form a variety of ETGs from very compact objects (as spectroscopically confirmed, Kriek et al. 2009; van Dokkum et al. 2009) to more extended ones (as present in the Mancini et al. sample). If high-redshift galaxies with lower masses are more turbulent (Förster Schreiber et al. 2009), and their mergers even more dispersion-dominated and dissipative, then the most compact ETGs would be low-mass ones. Such a trend is observed among the various samples of high-redshift spheroids (see Fig. 4 in Mancini et al. 2010). Faint extended stellar halos with high Sérsic indices are present, such as the one surrounding the massive kpc-sized core in the final ETG of model C1 (Fig. 4).

Young stellar clumps are seen in/around our ETGs. They could often be missed in observations. Those in the central body resemble the clumps observed in high-redshift ellipticals (Elmegreen et al. 2005). Outer clumps are seen around some ellipticals in the Mancini et al. sample. The outer clumps could become dwarf galaxies formed during the merger (tidal dwarf galaxies, Kroupa et al. 2010).

#### 4.4. Long-term evolution

High-redshift ETGs probably do not survive in the form of compact objects in the nearby Universe. They should grow mostly through dry minor mergers, which can increase their stellar sizes (Naab et al. 2009). In this dry process, the small and compact disk components remaining after high-redshift mergers (Fig. 1 at  $t = 625$ ) could undergo inefficient star formation (Martig et al.

2009) and persist as compact disks of residual gas and stars, as often found in the central kpc of nearby ellipticals (Young et al. 2008; Crocker et al. 2010).

### 5. CONCLUSION

The ISM is very turbulent and clumpy in high-redshift galaxies. Simulations of high-redshift mergers with cooling and enough resolution to develop turbulence and dense gas clouds show major differences compared to models with smooth, thermally supported disks:

- On-going mergers of representative high-redshift galaxies can have very irregular gaseous spheroids during the merger, with clumps and filaments throughout, instead of smooth rotating gas disks with long tidal tails as is common in low-redshift mergers.
- The gas velocity dispersion in these mergers becomes very high. At some stage, most of the gas kinetic energy is in the form of a three-dimensional velocity dispersion. Such mergers could take the appearance of dispersion-dominated galaxies with high gas dispersions and chaotic velocity fields.
- Turbulent and clumpy gas undergoes a violent and dissipative collapse in mergers. The final ETGs in these mergers are relatively compact, with high Sérsic indices and faint outer stellar halos.
- The masses and sizes of disk components that survive or re-form after major mergers are strongly reduced when the hydrodynamics of the cold turbulent ISM is taken into account. Large disks at high redshift should form mainly through cold accretion rather than mergers.

Mergers of primordial galaxies that are rich in turbulent and clumpy gas can undergo dispersion-dominated phases followed by dissipative collapse, leading to the formation of compact ETGs. Disk components cannot easily survive such mergers. If dust follows the scattering of gas in a three-dimensional clumpy distribution in/around the centrally collapsed system, star formation could be highly obscured like in Submillimeter Galaxies (Thronson et al. 1990).

We used HPC resources of CINES under GENCI allocation 2010-GEN2192. We acknowledge useful comments on the manuscript from Emmanuele Daddi, Eric Emsellem, Reinhard Genzel, David Law, and Paola Di Matteo.

### REFERENCES

- Agertz, O., Teyssier, R., & Moore, B. 2009, MNRAS, 397, L64  
 Bois, M., et al. 2010, MNRAS in press, arXiv:1004.4003  
 Bournaud, F., Duc, P.-A., Amram, P., Combes, F., & Gach, J.-L. 2004, A&A, 425, 813  
 Bournaud, F., Elmegreen, B. G., & Elmegreen, D. M. 2007, ApJ, 670, 237  
 Bournaud, F., Jog, C. J., & Combes, F. 2007, A&A, 476, 1179  
 Bournaud, F., Duc, P.-A., & Emsellem, E. 2008, MNRAS, 389, L8  
 Bournaud, F., et al. 2008, A&A, 486, 741  
 Bournaud et al. 2010, submitted to MNRAS  
 Brooks, A. M., Governato, F., Quinn, T., Brook, C. B., & Wadsley, J. 2009, ApJ, 694, 396  
 Cappellari, M., et al. 2009, ApJ, 704, L34  
 Ceverino, D., Dekel, A., & Bournaud, F. 2010, MNRAS, 440  
 Chilingarian, I., Di Matteo, P., Combes, F., Melchior, A.-L., & Semelin, B. 2010, A&A in press. arXiv:1003.3243  
 Conselice, C. J., Bershad, M.A., Dickinson, M., & Papovich, C. 2003, AJ, 126, 1183  
 Cox, T. J. 2004, Ph.D. Thesis, University of California, Santa Cruz

- Crocker, A. F., Bureau, M., Young, L. M., & Combes, F. 2010, submitted to MNRAS
- Daddi, E., et al. 2005, ApJ, 626, 680
- Daddi, E., et al. 2010, ApJ, 713, 686
- Dekel, A., Sari, R., & Ceverino, D. 2009, ApJ, 703, 785
- Dubois, Y., & Teyssier, R. 2008, A&A, 477, 79
- Elmegreen, D. M., Kaufman, M., Brinks, E., Elmegreen, B. G., & Sundin, M. 1995, ApJ, 453, 100
- Elmegreen, D. M., Elmegreen, B. G., & Hirst, A. C. 2004, ApJ, 604, L21
- Elmegreen, D. M., Elmegreen, B. G., & Ferguson, T. E. 2005, ApJ, 623, L71
- Elmegreen, D. M., Elmegreen, B. G., Ravindranath, S., & Coe, D. A. 2007, ApJ, 658, 763
- Elmegreen, B. G., Elmegreen, D. M., Fernandez, M. X., & Lemonias, J. J. 2009, ApJ, 692, 12
- Elmegreen, B. G., & Burkert, A. 2010, ApJ, 712, 294
- Epinat, B., et al. 2009, A&A, 504, 789
- Förster Schreiber, N. M., et al. 2009, ApJ, 706, 1364
- Genzel, R., et al. 2008, ApJ, 687, 59
- Jogee, S. et al. 2009, ApJ, 697, 1971
- Kriek, M., van Dokkum, P. G., Labbé, I., Franx, M., Illingworth, G. D., Marchesini, D., & Quadri, R. F. 2009, ApJ, 700, 221
- Kroupa, P., et al. 2010, A&A in press, arXiv:1006.1647
- Law, D. R., Steidel, C. C., Erb, D. K., Larkin, J. E., Pettini, M., Shapley, A. E., & Wright, S. A. 2009, ApJ, 697, 2057
- López-Sanjuan, C., et al. 2009, ApJ, 694, 643
- Lotz, J. M., Madau, P., Giavalisco, M., Primack, J., & Ferguson, H. C. 2006, ApJ, 636, 592
- Mancini, C., et al. 2010, MNRAS, 401, 933
- Martig, M., Bournaud, F., Teyssier, R., & Dekel, A. 2009, ApJ, 707, 250
- Naab, T., & Burkert, A. 2003, ApJ, 597, 893
- Naab, T., Johansson, P. H., & Ostriker, J. P. 2009, ApJ, 699, L178
- Overzier, R. A., Heckman, T. M., Schiminovich, D., Basu-Zych, A., Goncalves, T., Martin, D. C., & Rich, R. M. 2010, ApJ, 710, 979
- Puech, M. 2010, MNRAS in press
- Robertson, B., Bullock, J. S., Cox, T. J., Di Matteo, T., Hernquist, L., Springel, V., & Yoshida, N. 2006, ApJ, 645, 986
- Shapiro, K. L., et al. 2008, ApJ, 682, 231
- Springel, V., & Hernquist, L. 2005, ApJ, 622, L9
- Tacconi, L. J., et al. 2010, Nature, 463, 781
- Teyssier, R., Chapon, D., & Bournaud, F. 2010, ApJ in prep.
- Thronson, A. H., Majewski, S., Descartes, L., & Hereld, M. 1990, ApJ, 364, 456
- Trujillo, I., et al. 2006, MNRAS, 373, L36
- van Dokkum, P. G., Kriek, M., & Franx, M. 2009, Nature, 460, 717
- Weinzirl, T., Jogee, S., Khochfar, S., Burkert, A., & Kormendy, J. 2009, ApJ, 696, 411
- Young, L. M., Bureau, M., & Cappellari, M. 2008, ApJ, 676, 317